

Article

# Study on the Impact of Ammonia–Diesel Dual-Fuel Combustion on Performance of a Medium-Speed Diesel Engine

Hua Xiao <sup>1</sup>, Wenxuan Ying <sup>1,2</sup>, Aiguo Chen <sup>1,\*</sup>, Guansheng Chen <sup>2</sup>, Yang Liu <sup>1</sup>, Zhaochun Lyu <sup>1,2</sup>, Zengyin Qiao <sup>3</sup>, Jun Li <sup>1</sup>, Zhenwei Zhou <sup>1</sup> and Xi Deng <sup>4</sup>

<sup>1</sup> School of Naval Architecture and Ocean Engineering, Guangzhou Maritime University, Guangzhou 510725, China; xiaohua@gzmtu.edu.cn (H.X.); yingwx804@163.com (W.Y.); ly419355933@126.com (Y.L.); 13217681098@163.com (Z.L.); junli0201@163.com (J.L.); zw.zhou@hotmail.com (Z.Z.)

<sup>2</sup> School of Materials and Energy, Guangdong University of Technology, Guangzhou 510006, China; chengs@gdut.edu.cn

<sup>3</sup> R & D Department, Guangzhou Diesel Engine Factory Co., Ltd., Guangzhou 510370, China; 15200131645@163.com

<sup>4</sup> Department of Architecture, The University of Hong Kong, Hong Kong SAR, China; dengxi@hku.hk

\* Correspondence: chenaigu@126.com

**Abstract:** The combustion of diesel fuel in internal combustion engines faces challenges associated with excessive emissions of pollutants. A direct solution to this issue is the incorporation of cleaner energy sources. In this study, a numerical model was constructed to investigate the characteristics of ammonia–diesel dual-fuel application in a medium-speed diesel engine. Effects of ammonia–diesel blending ratios on engine performance and emissions were investigated. The results indicate that for this engine model, the optimal diesel energy ratio is about 22%. When the diesel energy ratio is less than 22%, the engine's output performance is significantly affected by the diesel energy ratio, while above 22%, the influence of the intake becomes more pronounced. When the diesel energy ratio is below 16%, the cylinder cannot reach combustion conditions. Diesel energy ratios below 22% can cause ammonia leakage. With increasing diesel energy ratio, the final emissions of carbon oxides increase. With a higher diesel energy ratio, NO emissions become lower. When the diesel fuel energy ratio exceeds 22%, the N<sub>2</sub>O emissions can be almost neglected, while below 22%, with poor combustion conditions inside the cylinder, the N<sub>2</sub>O emissions will increase.

**Keywords:** ammonia; diesel; dual fuel; simulation



**Citation:** Xiao, H.; Ying, W.; Chen, A.; Chen, G.; Liu, Y.; Lyu, Z.; Qiao, Z.; Li, J.; Zhou, Z.; Deng, X. Study on the Impact of Ammonia–Diesel Dual-Fuel Combustion on Performance of a Medium-Speed Diesel Engine. *J. Mar. Sci. Eng.* **2024**, *12*, 806. <https://doi.org/10.3390/jmse12050806>

Academic Editor: Leszek Chybowski

Received: 12 April 2024

Revised: 6 May 2024

Accepted: 7 May 2024

Published: 12 May 2024



**Copyright:** © 2024 by the authors. Licensee MDPI, Basel, Switzerland. This article is an open access article distributed under the terms and conditions of the Creative Commons Attribution (CC BY) license (<https://creativecommons.org/licenses/by/4.0/>).

## 1. Introduction

Global warming and pollution of the environment are among the major challenges facing the world today. Internal combustion engines, which utilize fossil fuels to directly convert the thermal energy of combustion into mechanical power [1], hold significant importance for human development and societal progress. However, traditional internal combustion engines using diesel as fuel emit substantial pollutants such as NO<sub>x</sub> and greenhouse gases like CO<sub>2</sub> and N<sub>2</sub>O [2]. These pollutants pose a significant threat to the health of people and to the environment. Scientists are turning their attention to renewable and clean fuels such as hydrogen, ammonia and methanol as the search for clean energy sources has become an urgent task [3–7]. Among these, ammonia, as a carbon-free fuel, offers advantages including easy storage, low cost and being environmentally friendly. It is gaining widespread attention from society [8–10]. However, ammonia also has drawbacks like low flame speed and high auto ignition temperature [11–13]. In addition, the emissions of NO<sub>x</sub> that occur during the combustion of ammonia and the release of unburned ammonia cannot be ignored [14,15]. To address these challenges, many studies have focused on the ammonia–diesel dual-fuel mode.

In the dual-fuel combustion mode known as Reactivity Controlled Compression Ignition (RCCI) [16], ammonia is considered an effective method for engine application. The RCCI mode blends high-octane fuel with low-octane fuel. The high-octane fuel serves as the main fuel in the fuel mix, while the low-octane fuel is utilized to control the process of mixed combustion [17,18]. Premixed low-reactivity fuel is injected into the cylinder through the intake manifold in RCCI combustion. This is followed by a direct injection of the highly reactive fuel into the cylinder. This concept aligns with the low reactivity characteristics of ammonia [19]. Reiter et al. [20,21] studied the combustion characteristics of ammonia–diesel dual-fuel in engines. The results indicate that the optimal operating range for the dual fuel process requires a diesel energy content between 40% and 60%, with increasing ammonia content resulting in longer ignition delays and lower peak combustion pressures. Yousefi et al. [22] found that as the ammonia energy fraction increases, combustion efficiency decreases significantly, with corresponding increases in ammonia leakage and  $N_2O$  emissions. Tay et al. [23] discovered that NO emissions increase significantly when the ammonia energy content is greater than 60% in comparison to pure diesel fuel. Advanced ignition timing can be used to control unburned ammonia emissions. Zhou et al. [24] studied the different effects of low-pressure injection dual-fuel mode and high-pressure injection dual-fuel mode on a marine ammonia diesel dual-fuel engine. The results showed that the low-pressure injection mode has a higher indicated thermal efficiency, while the high pressure injection mode can significantly reduce the emissions.

Currently, researchers are further investigating the characteristics of ammonia–diesel dual-fuel (ADDF) combustion in internal combustion engines through various numerical simulations. Shin et al. [25] investigated a direct-injection ammonia ADDF combustion engine, determined the optimal timing of liquid ammonia and diesel fuel injection, and proposed direct injection to add moment to improve the slow flame speed of ammonia and reduce unburned ammonia. Qian et al. [26] established a CFD model to quantitatively analyze the formation processes of different types of NO<sub>x</sub> and optimize the fuel injection timing to improve combustion efficiency for a marine diesel engine with a cylinder diameter of 230 mm. Liu et al. [27] studied an ammonia diesel stratified injection (ADSI) mode and found that it had higher thermal efficiency than the original diesel engine, significantly reducing greenhouse gas (GHG) emissions. Nadimi et al. [28] used a one-dimensional model to calculate combustion characteristic indicators for ammonia–diesel engines, revealing that  $N_2O$  generated from ammonia combustion offset the reduction in CO<sub>2</sub> emissions. Therefore, diesel must be replaced with more than 35.9% of ammonia to reduce greenhouse gas emissions.

To further investigate the combustion mode of ammonia–diesel dual fuel with ammonia gas introduced into the intake manifold, this paper conducted numerical simulations on a medium-speed six-cylinder four-stroke engine. The combustion process of ammonia–diesel inside the sealed cylinder was considered, during the period from the closing of intake valve to the opening of exhaust valve. The paper investigates the effect of small variations in the energy fraction of the diesel on the performance and emissions of the engine.

## 2. Numerical Setup

Numerical simulations were performed using CHEMKIN 2023 R1 software [29]; for the direct injection (DI) engine model in the internal combustion engine (ICE) module, numerical simulations of the combustion process in an ammonia–diesel dual-fuel engine were conducted. The mixture of ammonia and air were injected into the cylinder through the intake manifold. Diesel fuel was injected through a fuel injector to simulate the combustion process between the closing of the intake valve and the opening of the exhaust valve. During the simulation, a simplified chemical mechanism for an ammonia/n-heptane mixture, consisting of 495 reactions and 74 species, proposed by Bowen Wang's team [30], was employed. This simplified mechanism has been verified to exhibit good consistency with detailed mechanisms, making it suitable for simulating engine combustion processes

with high computational efficiency. Since n-heptane exhibits combustion characteristics similar to diesel [17,25,27,30–32], it was chosen as a substitute for diesel.

$$AEF = \frac{m_{\text{ammonia}} \times LHV_{\text{ammonia}}}{\text{TotalEnergy}} \quad (1)$$

$m_{\text{ammonia}}$ —Mass of ammonia;

$LHV_{\text{ammonia}}$ —Lower heating value of ammonia;

Total Energy—Total energy of the fuel mix.

As the model includes the simulation of fuel injection, parameters for n-heptane liquid fuel need to be added to the mechanism, of which some of the parameters are shown in Table 1. The ammonia blending ratio in diesel fuel was calculated using the ammonia energy fraction (AEF) [22], as shown in Equation (1). Some parameters of ammonia fuel are also shown. The ammonia energy fraction is defined as the proportion of ammonia energy to the total engine fuel energy, where  $m_{\text{ammonia}}$  and  $LHV_{\text{ammonia}}$  represent the mass and lower heating value of the premixed fuel (ammonia); Total Energy represents the total energy provided by both fuels. In the experiment, 28% of diesel energy was used to ignite ammonia. In the present study, while keeping other conditions constant, numerical simulations were performed with diesel energy ratios of 10%, 16%, 22%, 28%, 34%, and 40%, to analyze the performance and emissions of an ammonia–diesel dual-fuel engine.

**Table 1.** Parameters for ammonia and n-heptane fuel.

Parameters	n-Heptane	Ammonia
Boiling Point (K)	371.5	239.7
Lower Heating Value (MJ/kg)	44.9	18.6
Critical Temperature (K)	540.2	405.55
Density (g/cm <sup>3</sup> )	0.683	0.000771
Vapor Pressure (Kpa)	5.33	857.5

### 3. Results and Discussion

#### 3.1. Model Verification

The model verification in this study was conducted on a Wärtsilä DF32 engine (Wärtsilä, Helsinki, Finland) [19]. Specific engine parameters are presented in Table 2. The experimental setup involved the injection of ammonia through the intake manifold. The ammonia was ignited with a small amount of diesel fuel. Numerical simulations were performed under conditions of an ammonia premix equivalence ratio of 0.7 and an initial cylinder pressure of 1.112 bar on an ammonia–diesel engine with an ammonia energy fraction of 72.16%. The validation of the pressure during the in-cylinder combustion process is shown in Figure 1. From the figure, it can be seen that the pressure curve obtained from the numerical simulation is generally consistent with the experimental curve, with the simulated pressure slightly lower than the experimental values in the later stages of combustion. However, the peak pressures in simulation and experiment are almost the same. The maximum error in cylinder pressure is about 8.4%. Considering that the simulation used a zero-dimensional model and mixed ammonia and air uniformly in the cylinder, there can be differences from the actual cylinder conditions during the experiment. In addition, n-heptane was used in the simulation to model the combustion characteristics of diesel fuel, which cannot fully explain the combustion differences caused by the various components in the actual diesel fuel, which inevitably leads to a certain degree of error. Overall, the combustion of ammonia–diesel dual-fuel engines can be represented by the established zero-dimensional model.

**Table 2.** Basic parameters of diesel unit.

Engine Specification	
Engine type	4 strokes
Bore (mm)	320
Stroke (mm)	400
Connecting rod (mm)	848
Compression ratio	16
Engine speed (rpm)	750
Intake valve close (IVC) (°CA)	−225
Exhaust valve open (EVO) (°CA)	140
Top dead center (TDC) (°CA)	0
Bottom dead center (BDC) (°CA)	180/−180
Number of nozzle holes	4
Nozzle hole diameter (mm)	0.2

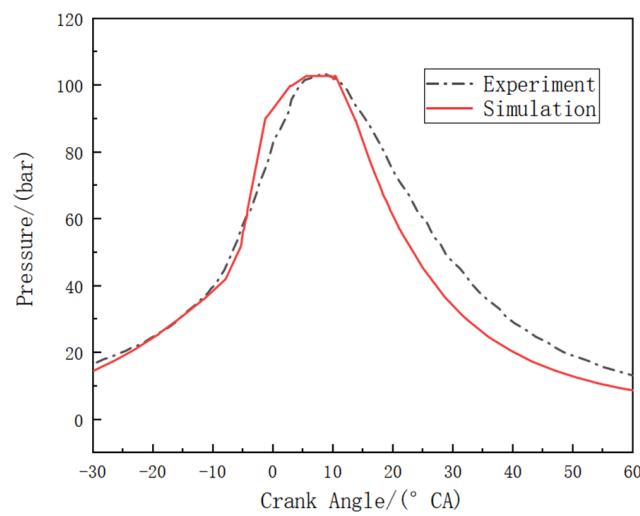


**Figure 1.** Comparison of simulated and experimental cylinder pressure values.

### 3.2. Effect of Diesel Energy Ratio on Engine Combustion Characteristics

#### 3.2.1. Cylinder Pressure and Temperature

Figures 2 and 3 show the curves of changes in cylinder pressure and cylinder temperature during combustion under different diesel energy ratios; Figure 4 provides a comparison of thermal efficiency and power.

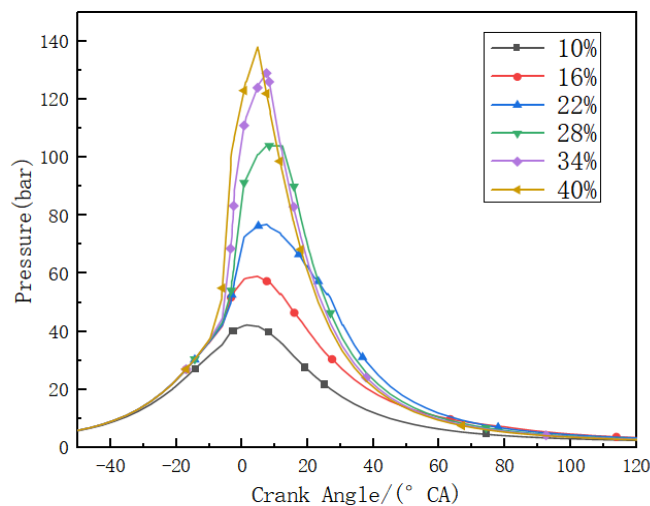


**Figure 2.** The cylinder pressure at different diesel energy ratios.

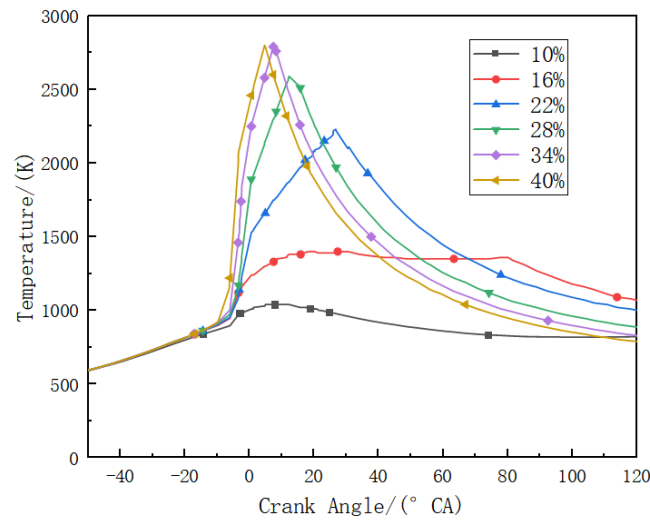


Figure 3. The cylinder temperature at different diesel energy ratios.

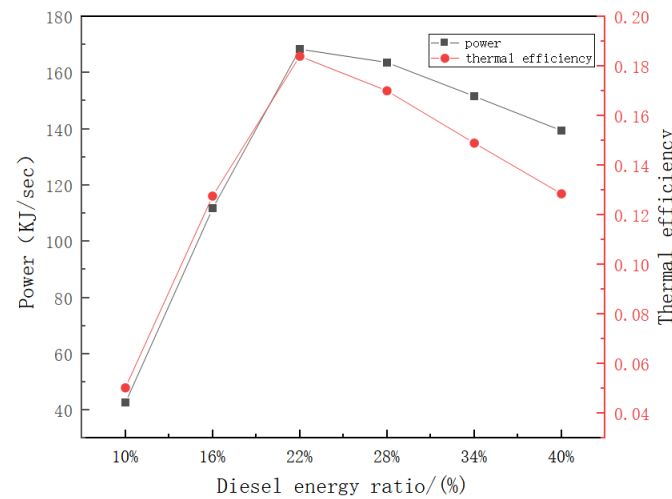


Figure 4. The power and thermal efficiency at different diesel energy ratios.

From Figures 2 and 3, it is evident that when the diesel energy ratio is 10% and 16%, the cylinder pressure and temperature are relatively low, the cylinder temperature shows a smooth trend, indicating that the cylinder did not reach combustion conditions when the diesel energy ratio was below 16%. When the energy ratio of the diesel engine exceeds 16%, the energy ratio of the diesel engine increases, the maximum pressure and maximum temperature in the cylinder increase, and the combustion in the cylinder starts earlier. This is due to the fact that ammonia has a high energy to ignite; an increase in the diesel energy ratio can make the cylinder reach ignition conditions more quickly, leading to a more rapid increase in cylinder temperature and an easier reaction. However, due to the excessive proportion of ammonia in this engine model, the combustion reaction rate is low, and when the diesel energy ratio gradually decreases, post-combustion phenomena become more severe [33]. At the same time, it can be observed that the changes in peak cylinder pressure and temperature are not significant during the transition from 34% to 40% diesel energy ratio. This is due to the limited cylinder volume. As a result, the air intake available for fuel combustion is insufficient, resulting in incomplete fuel combustion.

According to Figure 4, the influence of the diesel energy ratio on engine performance can be observed more intuitively: both power and thermal efficiency show a tendency to increase and then decrease. The power and thermal efficiency of the engine increase with increasing diesel fuel efficiency when the diesel fuel efficiency is less than 22%. Since ammonia is the main fuel during the combustion process, diesel fuel is mainly for the

ignition of the higher ignition energy content of ammonia, a diesel fuel energy ratio that is too low cannot effectively ignite the ammonia. When the diesel energy ratio exceeds 22%, both power and thermal efficiency gradually decrease with increasing diesel energy ratio. This indicates that when the diesel energy ratio is higher than 22%, the air content in the cylinder is low, deteriorating the combustion conditions, and the peak combustion performance occurs at a diesel energy ratio of 22%. This further indicates that when the diesel fuel-to-energy ratio is less than 22%, the output power of the engine is significantly affected by the diesel fuel-to-energy ratio, while when the diesel energy ratio exceeds 22%, the influence of the air content becomes more pronounced.

### 3.2.2. Ammonia Fuel Analysis

The variation of the ammonia fuel mass fraction at different diesel energy ratio conditions is shown in Figure 5. Ammonia is consumed slowly at first, followed by a rapid rate of consumption. Under conditions where the diesel energy ratio is greater than 22%, the ammonia is almost completely consumed with only a small amount of leakage. The more diesel is injected, the more intense the reaction inside the cylinder. However, under conditions where the diesel energy ratio is 10% and 16%, the total energy of the fuel mixture is low and normal combustion phenomena cannot occur inside the cylinder, resulting in a large amount of unreacted ammonia leakage, thereby causing serious environmental pollution.

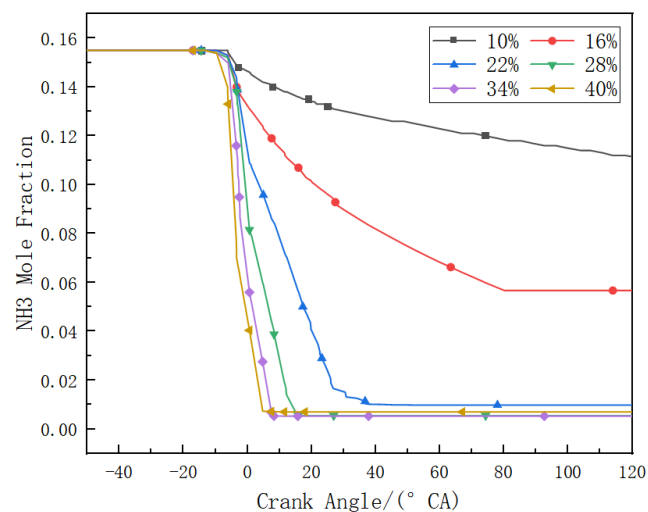


**Figure 5.** Mole fraction of NH<sub>3</sub> at different diesel energy ratios.

Figure 6 shows the overall reaction rate of the ammonia fuel at different diesel energy ratios. Overall, there is no apparent positive portion in the reaction rate, indicating a continuous consumption of ammonia during the combustion process. As the diesel energy ratio increases, the consumption rate of ammonia fuel increases significantly. The increase in the diesel energy ratio accelerates the increase in the cylinder temperature, which leads to an earlier start of the combustion and promotes the progress of the reactions related to the ammonia consumption-related species. This indicates that an increase in diesel quantity results in a more intense reaction of the ammonia fuel.

In order to gain a detailed understanding of the combustion process inside the cylinder, the specific parameters of the main elementary reactions involving the ammonia fuel are presented in Table 3. Numerical simulations provide the reaction rates of the main elementary reactions in which ammonia is involved during the combustion process in the cylinder of the engine. Figure 7 shows the curve of the reaction rates of the main elementary reactions involving ammonia during the combustion process at a diesel fuel energy ratio of 28% with respect to the crank angle. A positive reaction rate indicates the generation of ammonia in the elementary reaction, while a negative reaction rate indicates the consumption of ammonia in the elementary reaction.

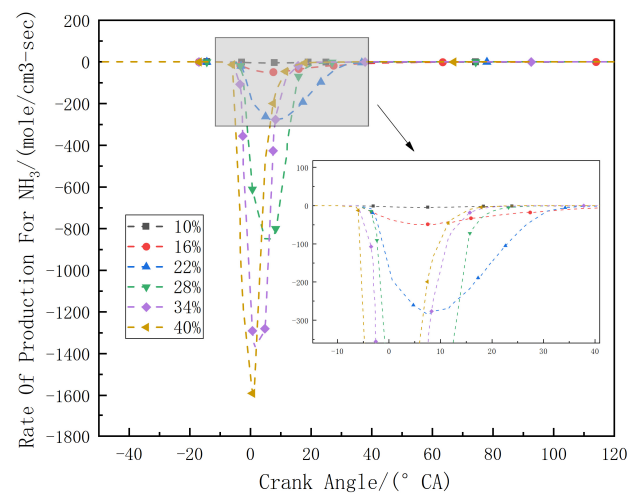


Figure 6. The total reaction rate of NH<sub>3</sub> at different diesel energy ratios.

Table 3. The major elementary reactions involving NH<sub>3</sub> during combustion.

Reaction Number	Elementary Reaction Formula
R187	$\text{NH}_3 \rightleftharpoons \text{NH}_2 + \text{H}$
R188	$\text{NH}_2 + \text{H}_2 \rightleftharpoons \text{NH}_3 + \text{H}$
R194	$2\text{NH}_2 \rightleftharpoons \text{NH}_3 + \text{NH}$
R230	$\text{NH}_3 + \text{O} \rightleftharpoons \text{NH}_2 + \text{OH}$
R231	$\text{NH}_3 + \text{OH} \rightleftharpoons \text{NH}_2 + \text{H}_2\text{O}$
R232	$\text{NH}_3 + \text{HO}_2 \rightleftharpoons \text{NH}_2 + \text{H}_2\text{O}_2$
R238	$\text{NH}_3 + \text{O}_2 \rightleftharpoons \text{NH}_2 + \text{HO}_2$
R372	$\text{HNCO} + \text{H}_2\text{O} \rightleftharpoons \text{NH}_3 + \text{CO}_2$
R392	$\text{NCO} + \text{NH}_3 \rightleftharpoons \text{HNCO} + \text{NH}_2$
R425	$\text{CH}_2(\text{S}) + \text{NH}_3 \rightleftharpoons \text{CH}_2\text{NH}_2 + \text{H}$

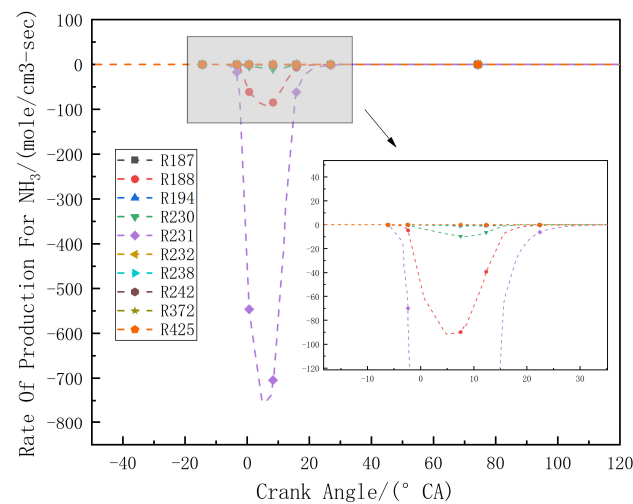
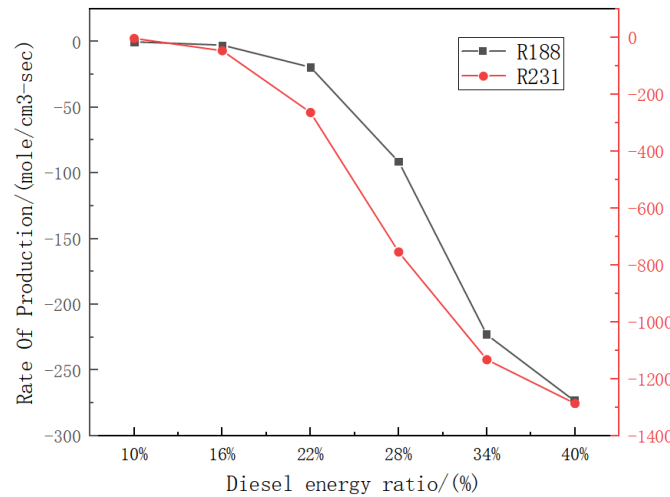


Figure 7. The reaction rates of the major elementary reactions involving NH<sub>3</sub> at a diesel energy ratio of 28%.

The study found that the primary elementary reactions mainly involve the consumption of ammonia and a significant consumption of hydroxyl and hydrogen radicals. These radicals promote the combustion process of the fuel and accelerate the release of energy. Among these reactions, R188 and R231 are the primary elementary reactions leading to ammonia consumption. It can be observed that the reaction rates of R188 and R231 both increase with the increase in the diesel energy ratio in combination with Figure 8. The

change in trend for R231 is particularly striking. During the process of increasing the diesel energy ratio from 10% to 40%, the reaction rate of elementary reaction R188 increases from 0.21 mole/cm<sup>3</sup>-s to 273.67 mole/cm<sup>3</sup>-s, while the reaction rate of elementary reaction R231 increases from 4.22 mole/cm<sup>3</sup>-s to 1286.29 mole/cm<sup>3</sup>-s. The oxygen in the cylinder mainly provides a large number of OH radicals through consumption reactions, thereby promoting ammonia consumption. With a higher diesel energy ratio, the temperature rise rate inside the cylinder is faster, leading to earlier consumption reactions of ammonia inside the cylinder.



**Figure 8.** The reaction rates of elementary reactions R188 and R231 at different diesel energy ratios.

### 3.2.3. Carbon Oxide Emissions

Figures 9 and 10 show the simulated curves of the variation of the mass fractions of CO and CO<sub>2</sub> at different diesel energy ratios. It can be seen that as the diesel energy ratio increases, both the production rate and the emissions of CO and CO<sub>2</sub> increase. This is attributed to the increased amount of carbon-based fuel injected. Considering that carbon in combustion originates entirely from diesel, a higher diesel energy ratio leads to higher emissions of carbon oxides. The production of CO exhibits a trend of initially increasing and then decreasing; the production of CO<sub>2</sub> exceeds that of CO. At a diesel energy ratio of 28%, the production of CO<sub>2</sub> is approximately four times that of CO.

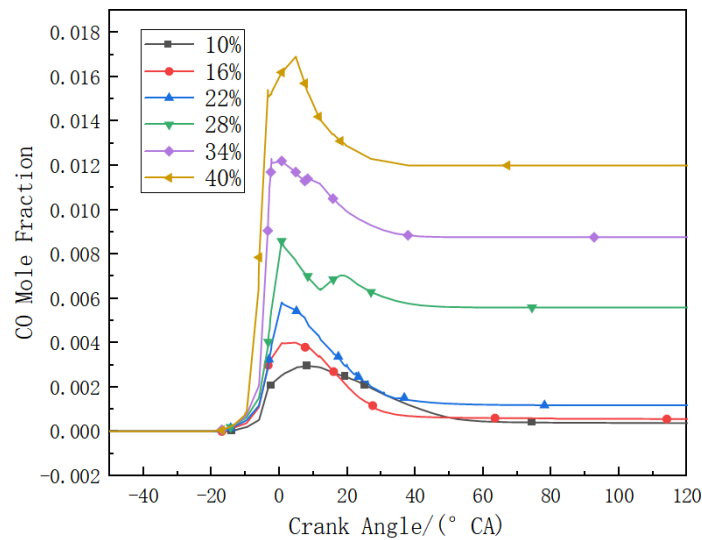


**Figure 9.** Mole fraction of CO at different diesel energy ratios.

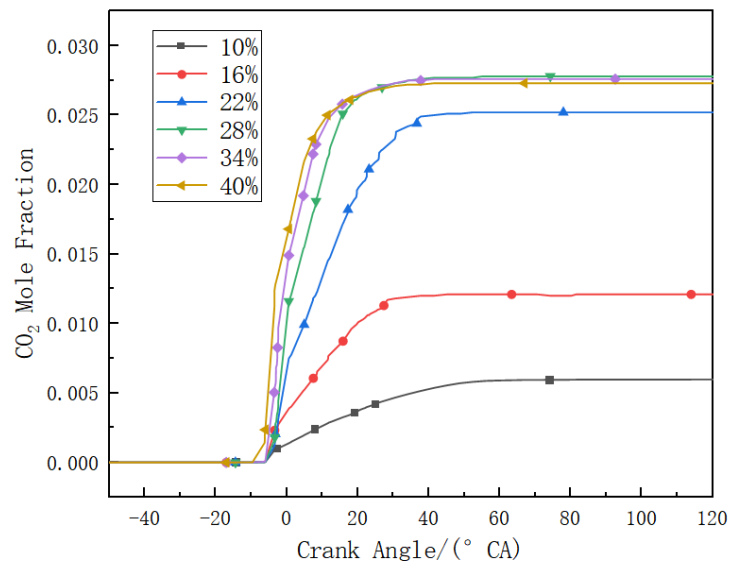


Figure 10. Mole fraction of CO<sub>2</sub> at different diesel energy ratios.

Tables 4 and 5 present the major elementary reactions involving CO and CO<sub>2</sub>, while Figures 11 and 12 illustrate the reaction rates of the major elementary reactions involving CO and CO<sub>2</sub> at a 28% diesel energy ratio. Similarly, positive and negative values indicate whether these reactions are generating or consuming CO and CO<sub>2</sub>.

Table 4. The major elementary reactions involving CO during combustion.

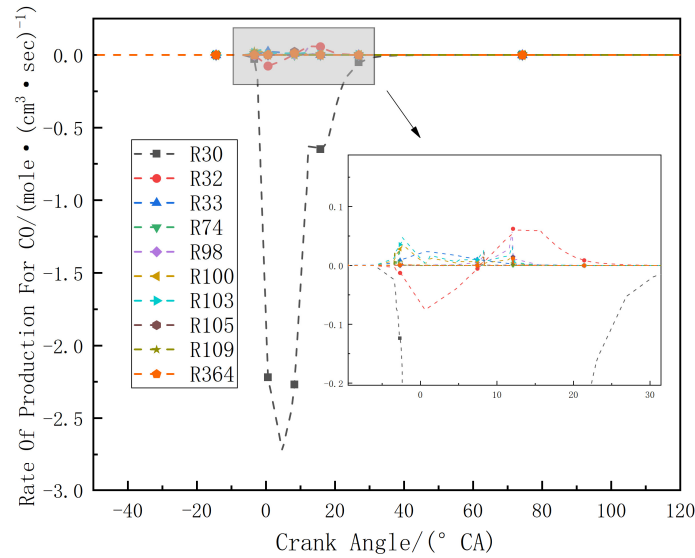
Reaction Number	Elementary Reaction Formula
R30	CO + OH $\rightleftharpoons$ CO <sub>2</sub> + H
R32	HCO + M $\rightleftharpoons$ H + CO + M
R33	HCO + O <sub>2</sub> $\rightleftharpoons$ CO + HO <sub>2</sub>
R98	CH <sub>2</sub> + CO(+M) $\rightleftharpoons$ CH <sub>2</sub> CO(+M)
R100	CH <sub>2</sub> CO + H $\rightleftharpoons$ CH <sub>3</sub> + CO
R103	CH <sub>2</sub> CO + OH $\rightleftharpoons$ CH <sub>2</sub> OH + CO
R105	HCCO + OH $\rightleftharpoons$ H <sub>2</sub> + 2CO
R109	HCCO + O <sub>2</sub> $\rightleftharpoons$ CO <sub>2</sub> + CO + H
R126	C <sub>2</sub> H <sub>2</sub> + O $\rightleftharpoons$ CH <sub>2</sub> + CO
R364	HNCO + H $\rightleftharpoons$ NH <sub>2</sub> + CO

Table 5. The major elementary reactions involving CO<sub>2</sub> during combustion.

Reaction Number	Elementary Reaction Formula
R28	CO + O(+M) $\rightleftharpoons$ CO <sub>2</sub> (+M)
R29	CO + O <sub>2</sub> $\rightleftharpoons$ CO <sub>2</sub> + O
R30	CO + OH $\rightleftharpoons$ CO <sub>2</sub> + H
R31	CO + HO <sub>2</sub> $\rightleftharpoons$ CO <sub>2</sub> + OH
R79	CH <sub>2</sub> + O <sub>2</sub> $\rightleftharpoons$ CO <sub>2</sub> + 2H
R101	CH <sub>2</sub> CO + O $\rightleftharpoons$ CH <sub>2</sub> + CO <sub>2</sub>
R109	HCCO + O <sub>2</sub> $\rightleftharpoons$ CO <sub>2</sub> + CO + H
R367	HNCO + O $\rightleftharpoons$ NH + CO <sub>2</sub>
R372	HNCO + H <sub>2</sub> O $\rightleftharpoons$ NH <sub>3</sub> + CO <sub>2</sub>
R395	CO + NO <sub>2</sub> $\rightleftharpoons$ NO + CO <sub>2</sub>

Through this study, it was found that during the combustion process, CO is primarily consumed. However, there are important reactions where it is also produced, like CO<sub>2</sub>, which is primarily produced. The consumption of CO and the generation of CO<sub>2</sub> are mainly achieved through the reaction R30: CO + OH  $\rightleftharpoons$  CO<sub>2</sub> + H, where CO is oxidized to CO<sub>2</sub>.

This clearly explains why the mole fraction curve of CO increases initially and then rapidly decreases with an increase in crankshaft angle and why the production of CO<sub>2</sub> is higher than that of CO.



**Figure 11.** Reaction rates of the major elementary reactions involving CO at a diesel energy ratio of 28%.

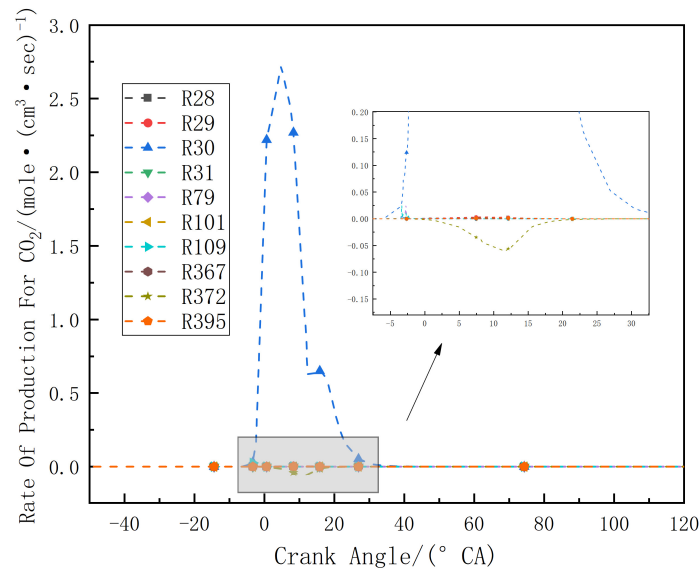


**Figure 12.** The reaction rates of the major elementary reactions involving CO<sub>2</sub> at a diesel energy ratio of 28%.

Additionally, it can be observed that in different diesel energy ratio conditions, CO does not completely react to form CO<sub>2</sub>; no other particularly intense reactions are evident in the major elementary reactions. The primary reason for this might be the setting of an equivalence ratio of 0.7 in this experiment, indicating that there is insufficient air in the combustion chamber to allow for complete ammonia reaction, thus resulting in overall lower thermal efficiency. The reaction rate of the elementary reaction R30 at different diesel energy ratios is shown in Figure 13. Under otherwise identical conditions, a higher diesel energy ratio corresponds to a higher reaction rate for R30, indicating a more intense reaction. It should also be noted that lowering the diesel energy ratio significantly reduces carbon dioxide emissions. This is because the combustion of pure ammonia does not produce carbon dioxide emissions.

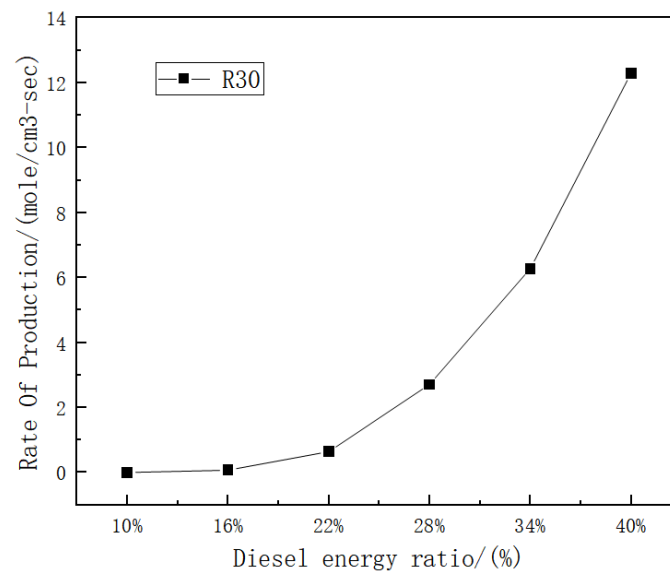


**Figure 13.** The reaction rates of elementary reaction R30 at different diesel energy ratios.

### 3.2.4. Nitrogen Oxide Emissions

Nitric oxide (NO) is considered a major precursor to ground-level ozone and atmospheric environmental pollution, while nitrous oxide ( $N_2O$ ), as a major driver of global climate change, is a significant greenhouse gas with an impact on temperature nearly 300 times greater than carbon dioxide. It takes approximately 120 years for  $N_2O$  to completely decompose in the atmosphere [34,35]. Figures 14 and 15, respectively, show the mole fractions of NO and  $N_2O$  under different diesel energy ratios. The higher the diesel energy ratio, the faster the rate of NO generation. However, the final emission of NO after combustion exhibits a trend of initially increasing and then decreasing with increasing diesel energy ratio. The maximum NO emission occurs at a diesel energy ratio of 22%. As mentioned earlier, combustion inside the cylinder is not ideal at diesel energy ratios of 10% and 16%. Therefore, it can be understood that under normal combustion conditions inside the cylinder, the higher the diesel energy ratio, the lower the NO emission. When ignition conditions are reached in the cylinder, diesel is ignited first. This generates a large amount of fuel-type NO, causing the NO content to rise sharply. The higher the diesel energy ratio, the faster the rate of NO formation. When the combustion ends, the temperature and pressure inside the cylinder begin to decrease, the remaining ammonia inside the cylinder gradually reduces NO, causing the NO level to decrease. Therefore, it can be observed that under conditions of lower diesel power ratio, the curve of NO generation reaches its peak and then decreases more slowly. However, even with low-temperature combustion, the emission of NO increases at lower diesel energy ratios due to the excessive amount of ammonia in the cylinder. The final emission of  $N_2O$  also exhibits a trend of initially decreasing and then increasing. However, in conditions where the diesel energy ratio is 10% and 16%, there is residual  $N_2O$  emission in the late stage of combustion, which can be due to incomplete combustion inside the cylinder, leading to too rapid a decrease in cylinder temperature. In conditions where the diesel energy ratio exceeds 28%, although there is a small amount of  $N_2O$  emission, its concentration is nearly an order of magnitude lower than that of NO emissions and can be considered negligible.

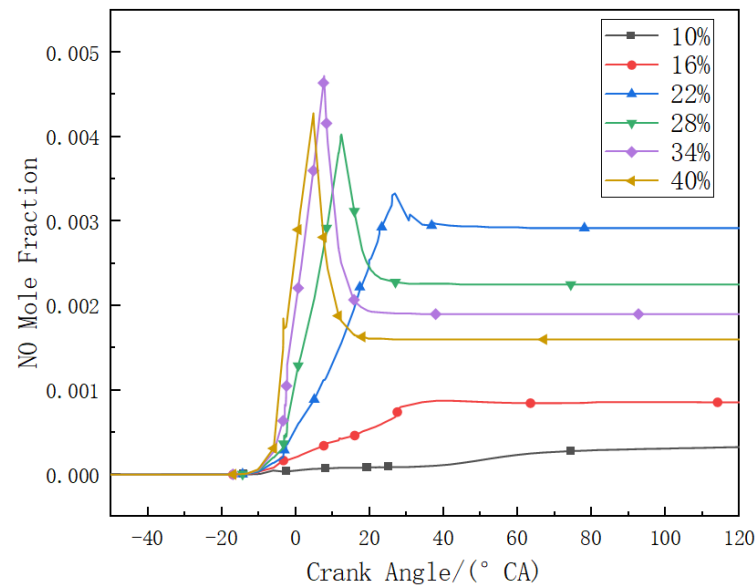


Figure 14. Mole fraction of NO at different diesel energy ratios.

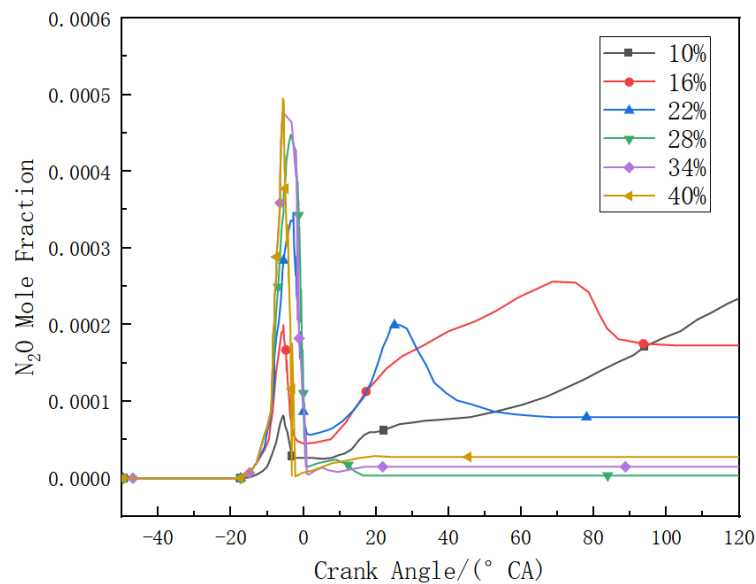
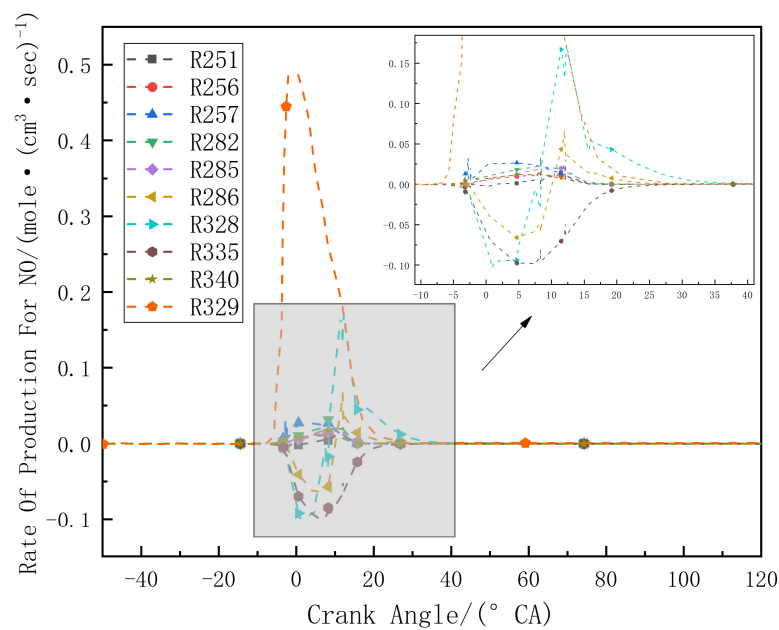


Figure 15. Mole fraction of N<sub>2</sub>O at different diesel energy ratios.

The major elementary reactions involving NO are shown in Table 6. The reaction rates of the major elementary reactions involving NO at a diesel fuel energy ratio of 28% are shown in Figure 16. It can be seen that NO is both produced and consumed during the combustion process. However, the production is predominant. Several reactions influence the NO content, including R286:  $\text{NO} + \text{O}(+\text{M}) \rightleftharpoons \text{NO}_2(+\text{M})$ , R328:  $\text{OH} + \text{NO} \rightleftharpoons \text{HONO}$ , R329:  $\text{H} + \text{NO}_2 \rightleftharpoons \text{OH} + \text{NO}$  and R335:  $\text{HNO} \rightleftharpoons \text{H} + \text{NO}$ . Among these, NO generation is primarily caused by R328 and R329. In the early stages of combustion, the forward reaction rate of R328, which tends to produce HONO, is relatively fast under high-temperature conditions as the cylinder temperature increases. In the later stages, when the OH concentration in the cylinder is high, it tends to favor the reverse reaction. In addition, around CA10, R286 and R335 contribute to the consumption of NO. As the combustion continues, ammonia reacts with OH and oxygen atoms through R230 and R231 to form amino  $\text{NH}_2$ , and then NO is destroyed by  $\text{NH}_2$ . However, this process typically occurs in the low-temperature range [36]; hence, the mole fraction of NO exhibits an initial increase, followed by a decreasing trend.

**Table 6.** The major elementary reactions involving NO during combustion.

Reaction Number	Elementary Reaction Formula
R251	$\text{NH} + \text{NO} \rightleftharpoons \text{N}_2\text{O} + \text{H}$
R256	$\text{N} + \text{OH} \rightleftharpoons \text{NO} + \text{H}$
R257	$\text{N} + \text{O}_2 \rightleftharpoons \text{NO} + \text{O}$
R282	$\text{HNO} + \text{H} \rightleftharpoons \text{NO} + \text{H}_2$
R285	$\text{NO} + \text{HO}_2 \rightleftharpoons \text{NO}_2 + \text{OH}$
R286	$\text{NO} + \text{O}(\text{+M}) \rightleftharpoons \text{NO}_2(\text{+M})$
R328	$\text{OH} + \text{NO} \rightleftharpoons \text{HONO}$
R329	$\text{H} + \text{NO}_2 \rightleftharpoons \text{OH} + \text{NO}$
R335	$\text{HNO} \rightleftharpoons \text{H} + \text{NO}$
R340	$\text{HNO} + \text{O}_2 \rightleftharpoons \text{NO} + \text{HO}_2$



**Figure 16.** The reaction rates of the major elementary reactions involving NO at a diesel energy ratio of 28%.

In conventional diesel engines, although combustion in the cylinder can produce  $\text{N}_2\text{O}$ , the amount produced is typically negligible. In ammonia–diesel dual-fuel engines, however, this issue must be considered because  $\text{N}_2\text{O}$  formation is one of the primary concerns associated with ammonia combustion. At low temperatures,  $\text{NO}_2$  reacts with ammonia to form  $\text{N}_2\text{O}$ . However, as the cylinder temperature increases under high-temperature conditions,  $\text{N}_2\text{O}$  is reduced back to  $\text{N}_2$ . Reaction R294 plays a dominant role in the reduction of  $\text{N}_2\text{O}$  to  $\text{N}_2$ , as shown in Figure 17. Table 7 shows the main elementary reactions of  $\text{N}_2\text{O}$  during combustion. Overall,  $\text{N}_2\text{O}$  is primarily consumed during the combustion process. When the diesel energy ratio is less than 28%, the temperature in the cylinder decreases after combustion; at this point, ammonia reacts to produce  $\text{N}_2\text{O}$  again. Therefore, in Figure 16, it can be seen that when the diesel energy ratio is below 28%, the  $\text{N}_2\text{O}$  content gradually increases in the later stages of combustion; moreover, the lower the diesel energy ratio, the higher the  $\text{N}_2\text{O}$  content.

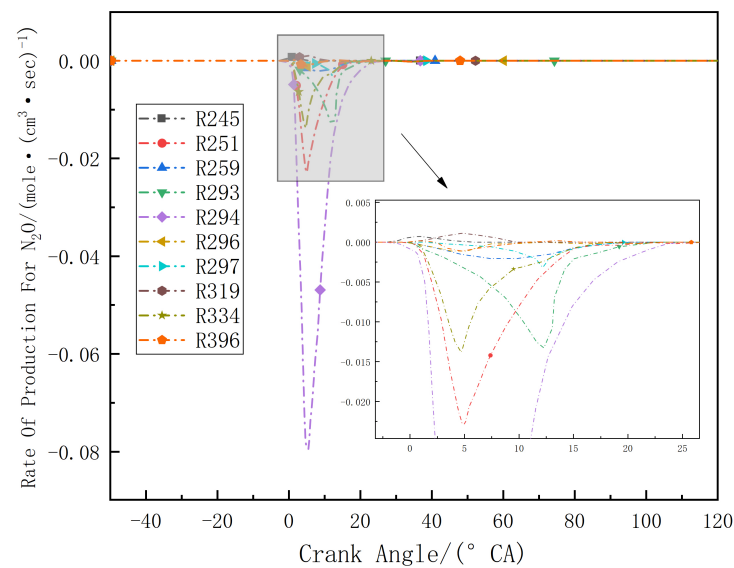


**Figure 17.** The reaction rates of the major elementary reactions involving N<sub>2</sub>O at a diesel energy ratio of 28%.

**Table 7.** The major elementary reactions involving N<sub>2</sub>O during combustion.

Reaction Number	Elementary Reaction Formula
R245	$\text{NH}_2 + \text{NO}_2 \rightleftharpoons \text{N}_2\text{O} + \text{H}_2\text{O}$
R251	$\text{NH} + \text{NO} \rightleftharpoons \text{N}_2\text{O} + \text{H}$
R259	$\text{NNH} + \text{O} \rightleftharpoons \text{N}_2\text{O} + \text{H}$
R293	$\text{N}_2\text{O}(\text{+M}) \rightleftharpoons \text{N}_2 + \text{O}(\text{+M})$
R294	$\text{N}_2\text{O} + \text{H} \rightleftharpoons \text{N}_2 + \text{OH}$
R296	$\text{N}_2\text{O} + \text{O} \rightleftharpoons 2\text{NO}$
R297	$\text{N}_2\text{O} + \text{OH} \rightleftharpoons \text{HO}_2 + \text{N}_2$
R319	$\text{N}_2\text{H}_2 + \text{NO} \rightleftharpoons \text{N}_2\text{O} + \text{NH}_2$
R334	$\text{N}_2\text{O} + \text{H}_2 \rightleftharpoons \text{N}_2 + \text{H}_2\text{O}$
R396	$\text{CO} + \text{N}_2\text{O} \rightleftharpoons \text{N}_2 + \text{CO}_2$

#### 4. Conclusions

In this study, numerical simulations of the combustion process were performed for an ammonia–diesel dual-fuel engine. It compared the performance of the engine, the combustion behavior and the pollutant emission characteristics within a small range of diesel fuel energy ratios (10–40%). The main conclusions of the research are as follows:

- (1) With the increase in the diesel energy ratio, the ignition inside the cylinder is significantly improved. However, both thermal efficiency and power show a trend of initial increase followed by a decrease. The peak occurs at a diesel energy ratio of about 22%. When the diesel energy ratio is below 16%, the mixture in cylinder cannot achieve ignition. Limited by the air intake available for fuel combustion inside the cylinder, the changes in cylinder temperature and pressure are not significant when the diesel energy ratio exceeds 34%. When the diesel energy ratio is less than 22%, the engine’s output performance is greatly affected by the diesel energy ratio, while above 22%, the influence of air intake becomes more pronounced.
- (2) When the diesel energy ratio is less than 22%, ammonia cannot be completely combusted, leading to ammonia leakage. As the diesel energy ratio increases, the reaction rate of ammonia becomes more intense. The main consumption reactions of ammonia are R231 and R188, and the injection of more diesel fuel will accelerate these reaction rates.
- (3) Considering that all of the carbon in the combustion come from diesel, the higher the amount of diesel is injected into the cylinder, the higher the final carbon oxides are

emitted. The interconversion between CO and carbon dioxide takes place primarily through the R30 reaction, in which CO is oxidized to form CO<sub>2</sub>. Therefore, the concentration of CO<sub>2</sub> is much higher than that of CO.

- (4) In terms of nitrogenous gas emissions, NO is the main pollutant primarily formed during the combustion process. It is mainly formed by the elementary reactions R328 and R329. With a higher diesel energy ratio, NO emissions are lower. In the early stages of combustion, when the cylinder temperature rises rapidly, R328 dominates. In the later stages of combustion, as cylinder temperature decreases and the concentration of OH radicals increases, R329 predominates and its reaction rate increases with the increase in the diesel energy ratio.
- (5) N<sub>2</sub>O primarily undergoes consumption during the combustion process, with the elementary reaction R294 playing a dominant role in this process. When the diesel energy ratio is less than 22%, the reduction in post-combustion temperature results in a decrease in the N<sub>2</sub>O consumption reaction rate, which is insufficient to offset the N<sub>2</sub>O formation. This results in even more N<sub>2</sub>O emissions.

**Author Contributions:** Conceptualization, H.X.; Methodology, Z.L. and X.D.; Software, Z.Q.; Data curation, Z.Z.; Writing—original draft, W.Y.; Visualization, Y.L.; Supervision, H.X., A.C. and G.C.; Project administration, J.L. All authors have read and agreed to the published version of the manuscript.

**Funding:** This work was supported by Scientific Research Capacity Improvement Project of Key Construction Discipline of Guangdong Province (No. 2022ZDJS099) and 2023 Basic and Applied Basic Research Project of Guangzhou Municipal Bureau of Science and Technology (No. SL2022A04J00794).

**Data Availability Statement:** Data are contained within the article.

**Conflicts of Interest:** Author Zengyin Qiao was employed by the company Guangzhou Diesel Engine Factory Co., Ltd. The remaining authors declare that the research was conducted in the absence of any commercial or financial relationships that could be construed as a potential conflict of interest.

## References

1. Johnsson, F.; Kjärstad, J.; Rootzén, J. The threat to climate change mitigation posed by the abundance of fossil fuels. *Clim. Policy* **2019**, *19*, 258–274. [[CrossRef](#)]
2. Yu, S.; Zheng, S.; Li, X. The achievement of the carbon emissions peak in China: The role of energy consumption structure optimization. *Energy Econ.* **2018**, *74*, 693–707. [[CrossRef](#)]
3. Xiao, H.; Valera-Medina, A.; Bowen, P.J. Modeling combustion of ammonia/hydrogen fuel blends under gas turbine conditions. *Energy Fuels* **2017**, *31*, 8631–8642. [[CrossRef](#)]
4. Xiao, H.; Valera-Medina, A.; Bowen, P.J. Study on premixed combustion characteristics of co-firing ammonia/methane fuels. *Energy* **2017**, *140*, 125–135. [[CrossRef](#)]
5. Valera-Medina, A.; Gutesa, M.; Xiao, H.; Pugh, D.; Giles, A.; Goktepe, B.; Marsh, R.; Bowen, P. Premixed ammonia/hydrogen swirl combustion under rich fuel conditions for gas turbines operation. *Int. J. Hydrogen Energy* **2019**, *44*, 8615–8626. [[CrossRef](#)]
6. Tang, Y.; Wang, Y.; Long, W.; Xiao, G.; Wang, Y.; Li, W. Analysis and enhancement of methanol reformer performance for online reforming based on waste heat recovery of methanol-diesel dual direct injection engine. *Energy* **2023**, *283*, 129098. [[CrossRef](#)]
7. Huang, Z.; Lyu, Z.; Luo, P.; Zhang, G.; Ying, W.; Chen, A.; Xiao, H. Effects of Methanol–Ammonia Blending Ratio on Performance and Emission Characteristics of a Compression Ignition Engine. *J. Mar. Sci. Eng.* **2023**, *11*, 2388. [[CrossRef](#)]
8. Xiao, H.; Howard, M.; Valera-Medina, A.; Dooley, S.; Bowen, P.J. Study on Reduced Chemical Mechanisms of Ammonia/Methane Combustion under Gas Turbine Conditions. *Energy Fuels* **2016**, *30*, 8701–8710. [[CrossRef](#)]
9. Kurien, C.; Mittal, M. Review on the production and utilization of green ammonia as an alternate fuel in dual-fuel compression ignition engines. *Energy Convers. Manag.* **2022**, *251*, 114990. [[CrossRef](#)]
10. Huang, S.Y.; Zhou, J.; Liu, S.J.; Peng, H.Y.; Yuan, X.Q. Continuous rotating detonation engine fueled by ammonia. *Energy* **2022**, *252*, 123911. [[CrossRef](#)]
11. Cai, T.; Zhao, D. Overview of autoignition and flame propagation properties for ammonia combustion. *AIAA J.* **2023**, *61*, 2754–2778. [[CrossRef](#)]
12. Kobayashi, H.; Hayakawa, A.; Somarathne, K.K.A.; Okafor, E.C. Science and technology of ammonia combustion. *Proc. Combust. Inst.* **2019**, *37*, 109–133. [[CrossRef](#)]
13. Li, J.; Liu, X.; Che, H.; Liu, C.; Li, C. Facile construction of O-doped crystalline/non-crystalline g-C<sub>3</sub>N<sub>4</sub> embedded nano-homojunction for efficiently photocatalytic H<sub>2</sub> evolution. *Carbon* **2021**, *172*, 602–612. [[CrossRef](#)]
14. Chiong, M.C.; Chong, C.T.; Ng, J.-H.; Mashruk, S.; Chong, W.W.F.; Samiran, N.A.; Mong, G.R.; Valera-Medina, A. Advancements of combustion technologies in the ammonia-fuelled engines. *Energy Convers. Manag.* **2021**, *244*, 114460. [[CrossRef](#)]

15. Wang, W.; Herreros, J.M.; Tsolakis, A.; York, A.P. Ammonia as hydrogen carrier for transportation; investigation of the ammonia exhaust gas fuel reforming. *Int. J. Hydrogen Energy* **2013**, *38*, 9907–9917. [[CrossRef](#)]
16. Paykani, A.; Garcia, A.; Shahbakhhti, M.; Rahnama, P.; Reitz, R.D. Reactivity controlled compression ignition engine: Pathways towards commercial viability. *Appl. Energy* **2021**, *282*, 116174. [[CrossRef](#)]
17. Reitz, R.D.; Duraisamy, G. Review of high efficiency and clean reactivity controlled compression ignition (RCCI) combustion in internal combustion engines. *Prog. Energy Combust. Sci.* **2015**, *46*, 12–71. [[CrossRef](#)]
18. Kokjohn, S.L.; Hanson, R.M.; A Splitter, D.; Reitz, R.D. Fuel reactivity controlled compression ignition (RCCI): A pathway to controlled high-efficiency clean combustion. *Int. J. Engine Res.* **2011**, *12*, 209–226. [[CrossRef](#)]
19. Xu, L.; Xu, S.; Bai, X.-S.; Repo, J.A.; Hautala, S.; Hyvönen, J. Performance and emission characteristics of an ammonia/diesel dual-fuel marine engine. *Renew. Sustain. Energy Rev.* **2023**, *185*, 113631. [[CrossRef](#)]
20. Reiter, A.J.; Kong, S.C. Combustion and emissions characteristics of compression-ignition engine using dual ammonia-diesel fuel. *Fuel* **2011**, *90*, 87–97. [[CrossRef](#)]
21. Reiter, A.J.; Kong, S.C. Demonstration of Compression-Ignition Engine Combustion Using Ammonia in Reducing Greenhouse Gas Emissions. *Energy Fuels* **2008**, *22*, 2963–2971. [[CrossRef](#)]
22. Yousefi, A.; Guo, H.; Dev, S.; Liko, B.; Lafrance, S. Effects of ammonia energy fraction and diesel injection timing on combustion and emissions of an ammonia/diesel dual-fuel engine. *Fuel* **2022**, *314*, 122723. [[CrossRef](#)]
23. Tay, K.L.; Yang, W.; Li, J.; Zhou, D.; Yu, W.; Zhao, F.; Chou, S.K.; Mohan, B. Numerical investigation on the combustion and emissions of a kerosene-diesel fueled compression ignition engine assisted by ammonia fumigation. *Appl. Energy* **2017**, *204*, 1476–1488. [[CrossRef](#)]
24. Zhou, X.; Li, T.; Wang, N.; Wang, X.; Chen, R.; Li, S. Pilot diesel-ignited ammonia dual fuel low-speed marine engines: A comparative analysis of ammonia premixed and high-pressure spray combustion modes with CFD simulation. *Renew. Sustain. Energy Rev.* **2023**, *173*, 113108. [[CrossRef](#)]
25. Shin, J.; Park, S. Numerical analysis and optimization of combustion and emissions in an ammonia-diesel dual-fuel engine using an ammonia direct injection strategy. *Energy* **2024**, *289*, 130014. [[CrossRef](#)]
26. Qian, Y.; Sun, Y.; Gong, Z.; Meng, S.; Wei, X.; Tang, B.; Wan, J. Study on the impact mechanism of ammonia energy fraction on in-cylinder combustion and pollutant generation under wide operation conditions of medium-speed diesel engines. *Fuel* **2024**, *360*, 130617. [[CrossRef](#)]
27. Liu, L.; Wu, J.; Liu, H.; Wu, Y.; Wang, Y. Study on marine engine combustion and emissions characteristics under multi-parameter coupling of ammonia-diesel stratified injection mode. *Int. J. Hydrogen Energy* **2023**, *48*, 9881–9894. [[CrossRef](#)]
28. Nadimi, E.; Przybyła, G.; Lewandowski, M.T.; Adamczyk, W. Effects of ammonia on combustion, emissions, and performance of the ammonia/diesel dual-fuel compression ignition engine. *J. Energy Inst.* **2023**, *107*, 101158. [[CrossRef](#)]
29. CHEMKIN-PRO 15131; Reaction Design: San Diego, CA, USA, 2013.
30. Wang, B.; Dong, S.; Jiang, Z.; Gao, W.; Wang, Z.; Li, J.; Yang, C.; Wang, Z.; Cheng, X. Development of a reduced chemical mechanism for ammonia/n-heptane blends. *Fuel* **2023**, *338*, 127358. [[CrossRef](#)]
31. Liu, L.; Wu, Y.; Wang, Y. Numerical investigation on the combustion and emission characteristics of ammonia in a low-speed two-stroke marine engine. *Fuel* **2022**, *314*, 122727. [[CrossRef](#)]
32. Kolaitis, D.I.; Founti, M.A. On the assumption of using n-heptane as a “surrogate fuel” for the description of the cool flame oxidation of diesel oil. *Proc. Combust. Inst.* **2009**, *32*, 3197–3205. [[CrossRef](#)]
33. Wang, B.; Wang, H.; Hu, D.; Yang, C.; Duan, B.; Wang, Y. Effect of different ammonia mixing methods for diesel ignition on combustion and emission performance of high pressure common rail engine. *J. Energy Inst.* **2023**, *111*, 101402. [[CrossRef](#)]
34. Yao, Z.; Wei, Y.; Liu, C.; Zheng, X.; Xie, B. Organically fertilized tea plantation stimulates N<sub>2</sub>O emissions and lowers NO fluxes in subtropical China. *Biogeosciences* **2015**, *12*, 5915–5928. [[CrossRef](#)]
35. Ravishankara, A.R.; Daniel, J.S.; Portmann, R.W. Nitrous Oxide (N<sub>2</sub>O): The Dominant Ozone-Depleting Substance Emitted in the 21st Century. *Science* **2009**, *326*, 123–125. [[CrossRef](#)]
36. Lee, G.W.; Shon, B.H.; Yoo, J.G.; Jung, J.H.; Oh, K.J. The influence of mixing between NH<sub>3</sub> and NO for a De-NO<sub>x</sub> reaction in the SNCR process. *J. Ind. Eng. Chem.* **2008**, *14*, 457–467. [[CrossRef](#)]

**Disclaimer/Publisher’s Note:** The statements, opinions and data contained in all publications are solely those of the individual author(s) and contributor(s) and not of MDPI and/or the editor(s). MDPI and/or the editor(s) disclaim responsibility for any injury to people or property resulting from any ideas, methods, instructions or products referred to in the content.